The Effect of Water Absorbent Polymer Beads on Fiber Reinforced Self-Compacting Concrete Exposed to Fire Flame

Noor Amer Mohamad Karem
Department of Civil Engineering, University of Baghdad, Baghdad, Iraq
noor.Aamer2301@coeng.uobaghdad.edu.iq (corresponding author)

Hadeel Khalid Awad
Department of Civil Engineering, University of Baghdad, Baghdad, Iraq
hadeel.kalid@coeng.uobaghdad.edu.iq

Received: 15 July 2025 | Revised: 7 August 2025 and 27 August 2025 | Accepted: 2 September 2025

 DOI: https://doi.org/10.48084/etasr.13423

ABSTRACT

Developing concrete that combines high mechanical efficiency with strong thermal resistance is essential to address the challenges of elevated temperatures and repeated mechanical stress. In this study, the performance of Self-Compacting Concrete (SCC) was improved using two techniques. First, Basalt Fibers (BF) were added due to their excellent thermal resistance. Second, Water-Absorbing Polymer Beads (WAPB) were incorporated at 3%, 4%, and 5% of the cementitious material weight to enhance the residual mechanical strength of SCC after fire exposure. The WAPB served two main functions. Initially, they provided internal curing by gradually releasing the absorbed water (after 24 h of pre-soaking) to sustain hydration after casting, and secondly their shrinkage created voids that acted as thermal insulators, reducing the risk of explosive spalling at 300 °C, 500 °C, and 700 °C. The objective was to investigate how BF and WAPB affect the SCC strength after fire exposure. The results showed that higher WAPB content improved the residual mechanical strength at elevated temperatures. Specifically, the residual compressive strengths were 32.91%, 36.95%, 41.89%, and 46.84%; the residual tensile strengths were 24.94%, 27.71%, 29.51%, and 31.42%; and the residual flexural strengths were 24.70%, 27.19%, 28.73%, and 30.33% for mixes BF0.4, BF0.4+P3, BF0.4+P4, and BF0.4+P5, respectively. All mixes contained 0.4% BF by volume, with WAPB ranging from 0% to 5% by cementitious material weight.

Keywords-self-compacting concrete; basalt fiber; thermal conductivity; water absorbent polymer

I. INTRODUCTION

The developments in construction engineering involve new types of concrete with different compositions, characteristics, and performance. Examples include SCC, known for its ability to fill molds without vibration [1-3]; foamed concrete, recognized for its lightweight and thermal insulation properties [4, 5]; and Reactive Powder Concrete (RPC), which shows excellent compressive strength and environmental resistance [6, 7]. Japan developed SCC in the 1980s that flows more efficiently than traditional concrete [8, 9]. It can be placed and compacted without vibration because it exhibits high deformability and resistance to segregation in its fresh state [10-12]. Adding fibers to self-compacted concrete improves its tensile and flexural strength after hardening, but it can negatively affect the workability when the former are fresh [13, 14]. Authors in [15-17] indicated that BF greatly enhances the split tensile strength and reduces the crack width in concrete, effectively improving the strength and damage resistance when used in calculated proportions. What makes BF superior to steel fibers is not only their mechanical properties, but also their environmental sustainability and cost-efficiency [18]. The production of BF requires less energy and produces lower CO_2 emissions, making them an eco-friendly option [19]. Therefore, BF are a great choice for improving the structural performance, environmental sustainability, and cost-effectiveness, suitable for modern projects aiming to balance performance with green practices [20]. Besides improving the flexural and tensile strength post-hardening, BF also increase the residual mechanical strength after exposure to high temperatures because they act as good thermal insulators and possess high thermal resistance [21-24]. Basalt rock fibers have desirable traits, such as a high melting point, compatibility with cementitious mixes, high tensile strength, and long-term durability [25]. Developing SCC that can withstand harsh conditions, like fire and high temperatures, has become essential to enhance the crack resistance and residual strength after heat exposure, especially since SCC is more heat-sensitive than ordinary concrete [26, 27]. Authors in [28] examined the residual compressive and tensile strengths of SCC after gradual

cooling from high temperatures. The results showed a negligible increase in the residual compressive strength at 150 °C, but at 300 °C, the compressive strength dropped to 20.27% and the tensile strength decreased by 50% at temperatures between 450 °C and 600 °C. Authors in [29] observed that the residual compressive strength of SCC declined when heated up to 650 °C. The exposure to high temperatures causes concrete deterioration; for example, with 0.25% BF, the concrete had a compressive strength of 71.3 MPa at 300 °C, slightly higher than the 70.7 MPa of unreinforced concrete. The addition of 0.5% BF significantly improved the performance at 600 °C. Residual strengths with varying BF percentages ranged from 28.4% to 34.3%. In comparison to unreinforced concrete, adding 0.5% BF reduced the thermal degradation and increased the residual strength more than 0.25% fiber ratio. Different polymers, like sheets [31], beads [32, 33], fibers [34], emulsion latex [35, 36], and bars [37], have been used. Internally curing concrete with polymer beads [38] has gained interest due to its role in increasing the strength and performance. As explained in [39], internal curing involves keeping concrete moist internally for longer than usual, using water-absorbing polymer granules to offset the moisture loss during curing in dry or hot conditions. This process reduces the self-shrinkage and maintains rehydration, sustaining the strength under high temperatures. According to [40], WAPB in SCC was achieved by pre-soaking the polymer in water before mixing, allowing continued hydration by releasing the internal water. The effect of air curing also influenced the development of the compressive strength, with 5% polymer beads relative to cement weight found to be optimal. Excessive amounts lowered strength. As shown in [41], adding SAP beads caused a 25.5% reduction in split tensile strength after three days due to delayed hydration and void formation from the water release. Similarly, authors in [42] added 5% pre-soaked WAPB, which increased 28-day compressive strength by 13%-15%, while water-cured samples saw a 10%-12% decrease due to the excessive water absorption causing internal damage. In [32], WAPB were used at ratios of 5%, 10%, 15%, and 20% of the cement weight with the aim of evaluating their effect on the compressive strength of concrete under two types of curing: water curing and air curing (after 7 days of initial water curing followed by air exposure). The optimal content, which achieved the best compressive strength, was 5%, with a value of 21 MPa at 28 days of air curing, higher than the reference specimens that had a strength of 20 MPa under air curing conditions. In contrast, at 5% of polymer beads and underwater curing, the compressive strength decreased to 18.5 MPa in 28 days, a reduction of 7. 7.5% compared to the reference mix at 28 days. This finding indicates that the polymer beads were more effective in air curing than in water curing for all polymer- containing mixes. The decreases are explained by the fact that internal curing provided by the polymer beads through their gradual and continuous release of the water content enhances the hydration reaction at later ages. Conversely, in water curing, the polymer beads continue to absorb water from the external environment until they reach their maximum limit, at which point they rupture and leave the internal voids that weaken the concrete structure. Despite the advantages of SCC in modern construction, it remains sensitive to high temperatures, even when reinforced with BF that improve its thermal resistance. Therefore, it has become necessary to enhance the latter by developing improved mixes that incorporate polymer beads to boost the strength, reduce the spalling caused by capillary water vapor pressure, and minimize the cracking after fire exposure. Although several studies have explored concrete reinforced with various fibers, the combined effect of fire exposure on SCC modified with water-absorbing polymer beads and reinforced with BF remains underexplored. The objective of this research is to evaluate the impact of WAPB on the fresh and some hardened mechanical properties of BF-reinforced SCC before and after exposure to different burning temperatures for 1 h, aiming to develop more fire- resistant concrete composites.

II. MATERIAL CHARACTERIZATION

A. Cement

Ordinary Portland Cement (OPC) [CEM.I. 42.5 N], known as ALMAS, was used in this experimental research. The results complied with those in [43]. Tables I and II provide a detailed description of OPC physical characteristics and chemical composition.

TABLE I. OPC CHEMICAL PROPERTIES

Oxides	**Content (%)**	**IQS, limits for CEM I-42.5 N**
(CaO)	63.33	-
(SiO2)	22.14	-
(Al2O3)	5.31	-
(Fe2O3)	2.89	-
(MgO)	3.39	Max (5) %
(SO3)	2.13	[SO3 ≤ 2.8] If C3A > 3.5
(L.O.I)	1.88	Max 4 %
(I.R)	0.92	Max 1.5 %
Calculated from Bogue's equations		
(C_3S)		49.68
(C_2S)		25.86
(C_3A)		9.18
(C_4AF)		8.78

TABLE II. OPC PHYSICAL PROPERTIES

Physical properties	**Results**	**IQS, limits for CEM.I. 42.5 N**
Surface area. (Blain method)	354	≥ 280
Setting time (Victa's Apparatus)		
Initial setting time (min)	155	≥ 45 min
Final setting time (h)	3:47	≤ 10 hrs
Compressive strength (MPa)		
2 days	18.60	≥ 10 MPa
28 days	44.71	≥ 42.5 MPa
Autoclave expansion (%)	0.19	≤ 0.8

B. Fine Aggregate (FA)

Table III presents the physical properties of the locally available sand, while Table IV provides the sieve analysis results, both in accordance with [43].

TABLE III. FA PHYSICAL PROPERTIES

Physical properties	**Results**	**[44]**
Specific gravity	2.59	-
Absorption ratio %	0.9	-
Sulphate amount	0.447	Max 0.5%
Dry rodded density (Kg/m^3)	1632	-

TABLE IV. FA SIEVE ANALYSIS

Sieve opening (mm)	Passing (%)	[43]
9.50	100	100
4.75	94	90 – 100
2.36	83	75 – 100
1.18	74	55 – 90
0.60	42	35 - 59
0.30	11	8 – 30
0.15	3	0– 10

C. Coarse Aggregate (CA)

Locally crushed CA with a nominal size of 10 mm was used. Its physical and chemical properties, along with the sieve analysis, are depicted in Tables V and VI and conform to [44].

TABLE V. CA PHYSICAL PROPERTIES

Properties	Results	[44]
Specific gravity	2.68	-
Absorption ratio %	0.5	-
Sulphate content	0.068	≤ 0.5
Dry rodded density (Kg/m^3)	1597	-

TABLE VI. CA SIEVE ANALYSIS

Sieve size (mm)	Passing (%)	Nominal size 10mm [44]
12.5	100	100
9.5	98	85-100
4.75	18	0-25
2.36	3	0-5

D. Silica Fume (SF)

All mixes included SF as a partial replacement of cement by 6%; SF complied with [45], as portrayed in Tables VII and VIII, correspondingly.

TABLE VII. SF PHYSICAL CHARACTERISTICS

Physical characteristics	Results	[45]
State	Amorphous	Sub-micron powder
Color	Grey	Grey
Specific surface area [m^2/g]	19	Min (15)
Strength activity index @ 7-day,	119	Min (105)
Retained on 45 µm sieve (No.325), %	8	Max (10)

TABLE VIII. SF CHEMICAL ANALYSIS

Oxide	Content (%)	[45]
SiO_2	92.14	Min 85%
Al_2O_3	<0.03	-
Fe_2O_3	0.98	-
CaO	0.65	-
MgO	0.73	-
TiO_2	<0.11	-
SO_4	0.58	-
P_2O_5	0.17	-
K_2O	1.03	-
LOI	3.56	Max 6%

E. Limestone (LM)

LM powder was used in the SCC mixtures for improving workability, density, and segregation resistance. Due to the particle size, which was smaller than 0.125 mm, Table IX shows the details.

TABLE IX. LM CHEMICAL COMPOSITION

Oxides	Content (%)
SiO_2	0.21
Fe_2O_3	3.33
Al_2O_3	0.03
CaO	48.28
MgO	3.94
SO3	0.07
L.O. I	43.12
IR	2.11

F. Superplasticizer (SP)

High-performance concrete SP (PC800), with a guidance dosage of 1 lt/100 kg to 2.9 lt/100 kg of cementitious materials was utilized. It functions as a high-range water-reducing SP and retarder. Hyperplastic was according to the requirements of specification type A and G [46]. Table X lists the properties of hyperplastic.

TABLE X. PROPERTIES OF PC800

Properties	Description
Form	Viscous liquid
Appearance/color	Light yellow
Chemical base	Modified polycarboxylate-based polymer
Specific gravity	1.06 g/cm^3 ± 0.02 g/cm^3
Dosage	1 lt/100 kg to 2.9 lt/100 kg of cementitious materials in the mix

G. Basalt Fibers

BF, also known as basalt rock fibers, are brown in color, as shown in Figure 1. They originate from volcanic rock and were used in this study with a length of 10 mm, a diameter of 15 µm, and a density of 2.6 g/cm³. Owing to their high elasticity, characterized by a modulus of elasticity of 75 GPa, tensile strength of 4.5 MPa, and elongation ratio of 3.15%, they were incorporated into the SCC mixture at a dosage of 0.4% of the total mix volume.

Fig. 1. BF.

H. Water Absorption Polymer Beads

WAPB are smart materials in the form of small, spherical polymers capable of absorbing water up to 100 times their own volume. For this study, they were pre-soaked in water 24 h prior to mixing. Figure 2 illustrates the appearance of the WAPB before and after immersion in water.

I. Water

Potable water, which conforms to [47], was used for the experiment.

Fig. 2. WAPB before soaking and after soaking.

J. Mix Proportions

A total of four SCC mixes were prepared. Each mix contained 510 kg/m³ of cement, 30.6 kg/m³ of SF (as a partial cement replacement), 60 kg/m³ of LM filler, 779 kg/m³ of sand, 870.6 kg/m³ of gravel, and a water-to-cementitious materials ratio (w/cm) of 0.29. An SP (PC800) was added at 2.9 L/100 kg of cementitious materials. All mixes included BF at 0.4% of the total concrete volume. The reference mix (BF0.4) contained only BF, while the other three mixes incorporated WAPB at 3%, 4%, and 5% of the cementitious material weight, labeled as BF0.4+P3, BF0.4+P4, and BF0.4+P5, respectively. The detailed proportions are presented in Table XI. All mixtures were designed to meet the SCC requirements specified in [48].

K. Fresh Concrete Properties

The workability of the fresh SCC mixes was evaluated using several standard tests: the slump flow test, V-funnel test, L-box test, and segregation resistance test, in accordance with [48]. The results are summarized in Table XII and illustrated in Figure 3, following the specifications in [49].

Fig. 3. Fresh tests. (a) Slump flow test, (b) V-funnel test, (c) L- Box test.

L. Hardened Concrete Testing

Mechanical and thermal tests were carried out on hardened SCC specimens. The compressive strength was measured using 10 × 10 × 10 cm cubes at 7, 28, and 56 days, with the results based on the average of three specimens per age, following the specifications of [49]. The splitting tensile strength was determined using 10 × 20 cm cylindrical specimens at the same ages, in line with [50]. The flexural strength was tested on 7.5 × 7.5 × 38 cm prisms using a one-point loading method, as specified in [51]. All mechanical tests were conducted with a hydromechanical testing machine of 2000 kN capacity and a 2.5 MPa/s loading rate. Additionally, the thermal conductivity was measured at 28 days using 10 cm × 10 cm × 10 cm cubes, in accordance with [58].

TABLE XI. MIX PROPORTION FOR SCC

Specimen	Cement (kg/m³)	SF (kg/m³)	LM (kg/m³)	Sand (kg/m³)	Gravel (kg/m³)	Water (kg/m³)	SP lt/100kg of cementitious materials	w/cm	BF by volume fraction (%)	WAPB by weight of cementitious material (%)
$BF_{0.4}$	510	30.6	60	779	870.6	156.6	2.9	0.29	0.4	0
$BF_{0.4}+P_3$	510	30.6	60	779	870.6	156.6	2.9	0.29	0.4	3
$BF_{0.4}+P_4$	510	30.6	60	779	870.6	156.6	2.9	0.29	0.4	4
$BF_{0.4}+P_5$	510	30.6	60	779	870.6	156.6	2.9	0.29	0.4	5

TABLE XII. FRESH PROPERTIES OF SCC

No	Mix ID	Fresh properties of SCC according to [48]				
		Slump flow (mm)	T_{500} (s)	V-funnel (s)	L- Box (h2/h1)	Sieve Segregation Index (SI) (%)
1	$BF_{0.4}$	716	9	15	0.88	11.76
2	$BF_{0.4}+P_3$	750	8	12.6	0.91	13.15
3	$BF_{0.4}+P_4$	772	7.4	11.1	0.92	14.42
Limits of [48]		SF1 (550-650) SF2 (660-750) SF3 (760-850)	VS 1 ≤ 2 VS 2 > 2	VF 1 ≤ 8 VF 2 (9-25)	PA 1 ≥ 0.8 PA 2 ≥ 0.8	SR 1 ≤ 20 SR 2 ≤ 15

M. Burning Procedure

Based on the methods reported in [52–54], all specimens intended for fire testing at 56 days were first cured in water for 28 days, followed by an additional 28 days of air curing in the laboratory. At 56 days, each specimen was placed in a cooled furnace measuring 3500 mm × 2000 mm × 900 mm, as shown in Figures 3(a) and 3(b). The furnace temperature was

monitored with a digital thermometer, as illustrated in Figure 3(c). The specimens were then exposed to fire flames at target temperatures of 300 °C, 500 °C, and 700 °C. The heating rate was controlled in accordance with [55] until the desired temperature was reached. Each specimen was maintained at the target temperature for 1 h, after which it was removed from the furnace and allowed to cool naturally to room temperature before testing.

(a) (b) (c)

Fig. 4. Burning process. (a) Placing the specimens in the furnace, (b) burning furnace, (c) digital thermometer.

III. RESULTS AND DISCUSSION

A. Fresh Properties of SCC

The fresh properties of the mixes are summarized in Table XII and Figure 3, following the specifications of [48]. The measured ranges were: a slump flow diameter of 716 mm – 787 mm, T500 9 s – 6.9 s, V-funnel 15 s – 9.8 s, L-box ratio 0.88–0.94, and SI 11.76%–15.51%. The reference mix containing only BF0.4 recorded the lowest slump flow diameter, L-box ratio, and SI among all mixes. Incorporating WAPB improved these results compared to BF0.4. The improvements increased with higher WAPB content. For mixes BF0.4+P3, BF0.4+P4, and BF0.4+P5, the slump flow increased by 4.75%, 7.82%, and 9.92%, respectively, while the L-box ratio increased by 3.41%, 4.55%, and 6.82%, and the SI increased by 11.82%, 22.62%, and 31.89%, compared with BF0.4. The enhancement in the flowability is attributed to the smooth, spherical shape of the polymer beads, which reduces the internal friction and decreases the interlocking effect between the BF and the aggregates [26, 56]. The T500 test results ranged from 9.9 s to 6.9 s, with the BF mixes showing higher values compared to those containing WAPB [13, 57]. However, adding polymer beads reduced the negative effect of BF on workability, as confirmed by the results in Table XII.

B. Mechanical Properties

1) Thermal Conductivity

As presented in Table XIII and Figure 5, the thermal conductivity coefficient (K value) of the SCC specimens ranged from 1.061 to 1.308 W/(m·K) at 28 days, measured on 10 cm × 10 cm × 10 cm cubes, in accordance with [58]. The addition of WAPB increased the thermal conductivity compared to the reference mix (BF0.4). At BF0.4+P3, the conductivity rose by 11.88%, while the highest increase was observed in BF0.4+P5, with a 23.28% rise over BF0.4. This trend can be explained by the dual effect of BF and polymer beads. BF contribute to thermal insulation by reducing the heat transfer through the concrete matrix. However, WAPB, once surrounded by hydration products, enhance heat transfer and raise the thermal conductivity as their content increases [59, 60].

TABLE XIII. THERMAL CONDUCTIVITY (W/M. K)

Mix	At 28 days
$BF_{0.4}$	1.061
$BF_{0.4}$+P_3	1.187
$BF_{0.4}$+P_4	1.248
$BF_{0.4}$+P_5	1.308

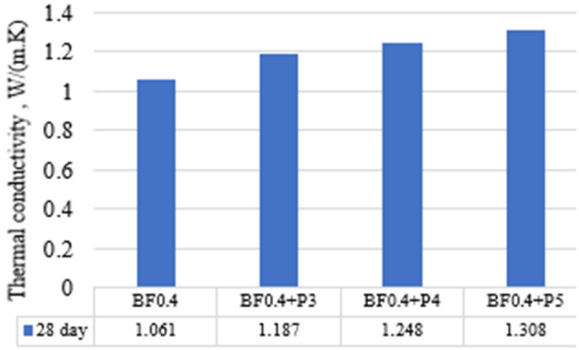

Fig. 5. Thermal conductivity.

2) Compressive Strength

The results of the compressive strength test on SCC cubes are presented in Table XIV and Figure 6, where the tests were conducted on two different groups of samples subjected to the same mixing and casting conditions. The first group was tested at 7 and 28 days of age under water-curing throughout the period. It showed a decrease in compressive strength compared to the reference samples, with reductions of 9.33%, 21.88%, and 28.72% for the mixtures BF0.4+P3, BF0.4+P4, and BF0.4+P5, respectively, compared to BF0.4 at 28 days. The reason is that the polymer beads WAPB formed voids in the concrete structure, reducing the overall density of the mass, which in turn decreased its compressive strength. As for the second group, it was prepared within the same batch, but a water curing period of 28 days was followed by an air curing period of an additional 28 days (up to 56 days of age). These samples also showed less compressive strength than the reference mix BF0.4, but the rate of improvement in strength compared to the 28-day age was higher. The increase rate in the samples BF0.4, BF0.4+P3, BF0.4+P4, and BF0.4+P5 belonging to the 56-day group was 9.41%, 15.53%, 22.30%, and 27.13%, respectively, compared to the decrease rate in the samples belonging to the first group at 28 days, which was 33.33%, 26.13%, 22.51%, and 18.21%. This indicates that there is a decrease in strength for the 28-day group, while the strength increases with the addition of polymer beads at 56 days. This behavior is due to the continuity of the internal curing resulting from the moisture provided by the polymer beads gradually during the air curing period, contributing to the formation of more hydration products and a denser concrete structure over time. This finding is consistent with those in [32].

TABLE XIV. COMPRESSIVE STRENGTH BEFORE BURNING, (MPA)

Mix	Water curing		Difference between 7 and 28 days (%)	Air curing	Difference between 28 and 56 days (%)
	7 days	28 days		56 days	
$BF_{0.4}$	47.19	62.92	33.33	68.84	9.41
$BF_{0.4}+P_3$	45.23	57.05	26.13	65.91	15.53
$BF_{0.4}+P_4$	40.12	49.15	22.51	60.11	22.30
$BF_{0.4}+P_5$	37.94	44.85	18.21	57.02	27.13

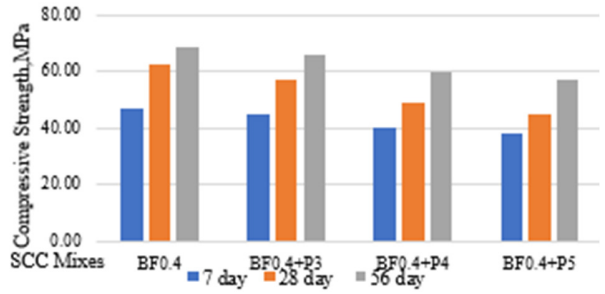

Fig. 6. Effect of WAPB on the compressive strength before burning.

The residual compressive strength of SCC is shown in Table XV and Figure 7 at 56 days after the burning process. The compressive strength decreases significantly with an increasing burning temperature (300 °C, 500 °C, and 700 °C), and it decreases further with an increasing WAPB%. An increase in the burning temperature has less impact on SCC 3%, 4%, and 5% WAPB specimens compared to the same specimens before burning. SCC specimens with 5% WAPB had the highest residual compressive strength at 300 °C, 500 °C, and 700 °C, respectively, and were the least affected by the heat rising after exposure to burning compared to the same mix before burning. This advantage is due to a greater content of internal voids that are caused by the shrinkage of WAPB after fully releasing the water content, which allows for more flexibility in the moisture movement, minimizes the stresses inside SCC, and reduces the explosive spalling [33].

TABLE XV. PERCENTAGE OF RESIDUAL COMPRESSIVE STRENGTH (%)

Mix	at 300 °C	at 500 °C	at 700 °C
$BF_{0.4}$	79.68	54.71	32.91
$BF_{0.4}+P_3$	84.7	59.71	36.95
$BF_{0.4}+P_4$	88.93	63.88	41.89
$BF_{0.4}+P_5$	93.53	67.81	46.84

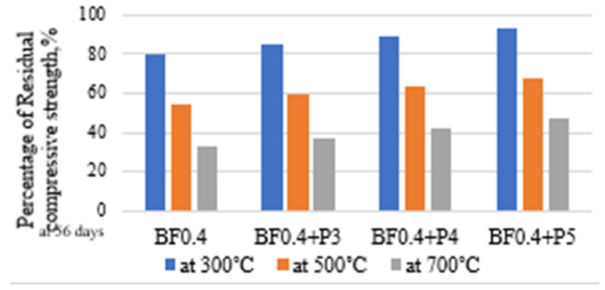

Fig. 7. Percentage of residual compressive strength after burning.

3) Splitting Tensile Strength

The results of the split tensile strength test for the SCC samples after 28 and 56 days (air-cured for 28 days after immersion in water for 28 days) are displayed in Table XVI and Figure 8. The introduction of polymer beads led to a decrease in the tensile strength. This decrease becomes more apparent when 5% of WAPB is used, resulting in a 36.91% reduction in the BF0.4+P5 samples after 28 days of water treatment compared to the BF0.4 samples. After completing the air curing, which is the second stage of treatment for the 56-day group, the increase rates in the samples BF0.4, BF0.4+P3, BF0.4+P4, and BF0.4+P5 were 9.92%, 13.42%, 19.89%, and 25.76%, respectively. Compared to the rate of decrease in the samples belonging to the 28-day group, which was 32.97%, 23.94%, 19.95%, and 17.74%, the decrease indicates a negative role of the polymer beads in contributing to the development of split tensile strength values under water treatment for the 28-day samples. Conversely, under air treatment conditions for 56 days, there was a positive effect on the split tensile strength. The explanation for this effect is the drying of the surroundings around the polymer, which forces the polymer beads to release all their water content and shrink, providing internal curing. The additional hydration products contributed to an increased density and improved bonding between the components of the cement paste, aggregate, and BF [33, 41].

TABLE XVI. SPLITTING TENSILE STRENGTH BEFORE BURNING (MPA)

Mix	Water curing		Difference between 7 and 28 days (%)	Air curing	Difference between 28 and 56 days (%)
	7 days	28 days		56 days	
$BF_{0.4}$	5.46	7.26	32.97	7.98	9.92
$BF_{0.4}+P_3$	4.93	6.11	23.94	6.93	13.42
$BF_{0.4}+P_4$	4.36	5.23	19.95	6.27	19.89
$BF_{0.4}+P_5$	3.89	4.58	17.74	5.76	25.76

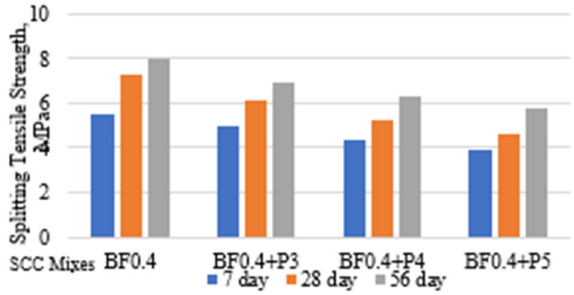

Fig. 8. Effect of WAPB on the splitting tensile strength before burning.

At 56 days (following 28 days of water curing and 28 days of air curing), the residual splitting tensile strength of the specimens was evaluated after fire exposure. The results showed that BF0.4+P5 achieved the highest residual tensile strength compared to the other mixes and also outperformed its pre-burning values. This improvement is attributed to the voids formed by the shrinkage of the polymer beads after releasing their water content. These voids act as thermal insulators, reducing the heat transfer within the concrete, and as channels for releasing capillary water vapor, thereby limiting the

explosive spalling at high temperatures. As a result, the adverse effects of the heat on the concrete matrix were reduced, helping to prevent the deterioration and minimize the cracking [33].

TABLE XVII. PERCENTAGE OF RESIDUAL TENSILE STRENGTH (%)

Mix	at 300 °C	at 500 °C	at 700 °C
$BF_{0.4}$	72.43	47.37	24.94
$BF_{0.4}+P_3$	76.62	49.93	27.71
$BF_{0.4}+P_4$	79.59	53.43	29.51
$BF_{0.4}+P_5$	80.38	54.17	31.42

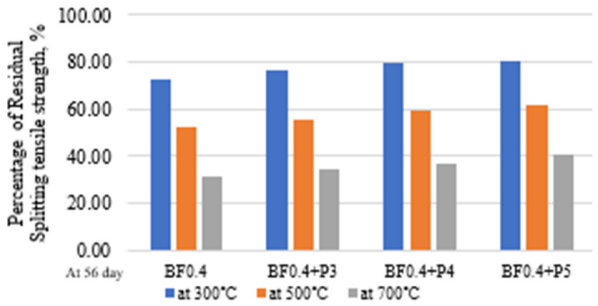

Fig. 9. Percentage of residual splitting tensile strength after burning.

4) Flexural Strength

The test results for the flexural strength of the SCC specimens at 7, 28, and 56 days (which were subjected to air curing for 28 days after being immersed in water for 28 days) are presented in Table XVIII. Figure 10 illustrates that increasing the proportion of WAPB by 3%, 4%, and 5% in the SCC resulted in a notable reduction in the flexural strength. For the BF0.4, BF0.4+P3, BF0.4+P4, and BF0.4+P5 specimens, the reduction rates were 33.33%, 24.22%, 21.35%, and 18.39%, respectively, at underwater curing at 28 days, relative to the increasing rate in the flexural strength for higher concentrations of WAPB in the specimens when the latter were exposed to air for the other 28 days (in 56 days) by (10.04, 14.36, 21.91, 26) for (0%, 3%, 4%, and 5%). WAPB, respectively, was higher due to the moisture provided from WAPB inside the SCC specimens, which was the reason for continuing the hydration processes at a later age, leading to denser concrete [61].

TABLE XVIII. FLEXURAL STRENGTH BEFORE BURNING (MPA)

Mix	Water curing		Difference between 7 and 28 days (%)	Air curing	Difference between 28 and 56 days (%)
	7 days	28 days		56 days	
$BF_{0.4}$	6.87	9.16	33.33	10.08	10.04
$BF_{0.4}+P_3$	6.11	7.59	24.22	8.68	14.36
$BF_{0.4}+P_4$	5.34	6.48	21.35	7.9	21.91
$BF_{0.4}+P_5$	4.84	5.73	18.39	7.22	26.00

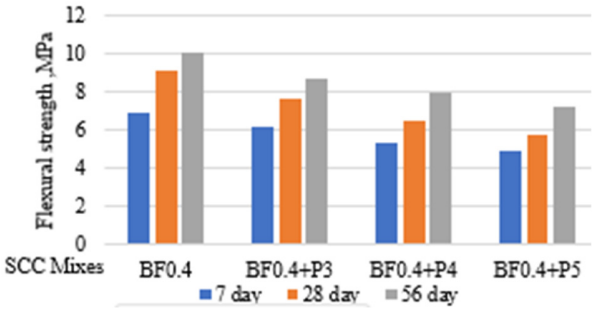

Fig. 10. Effect of WAPB on the flexural strength before burning.

Table XIV and Figure 11 provide the results of testing the SCC specimens for flexural strength 56 days after the burning process. The behavior of concrete in the flexural strength test after the exposure to fire flames resembles its behavior in the compressive test, as the WAPB preserved the residual flexural strength of the concrete after the exposure to fire flames. This was particularly evident with the BF0.4+P5 specimens, which had the highest residual flexural strength compared to the same mixes before the exposure to the fire flames. This is due to the increased content of WAPB in the specimens, which led to the formation of air voids that contributed to reducing the heat transfer within the concrete structure. These voids act as a relative thermal insulator, which reduces the severity of the thermal gradient between the layers of concrete and minimizes the spread of micro-cracks. As a result, the SCC specimens containing higher ratios of WAPB showed a better ability to retain their residual strength after exposure to burning compared to the other samples.

TABLE XIX. PERCENTAGE OF RESIDUAL FLEXURAL STRENGTH (%)

Mix	at 300 °C	at 500 °C	at 700 °C
$BF_{0.4}$	69.15	43.75	24.70
$BF_{0.4}+P_3$	71.08	46.77	27.19
$BF_{0.4}+P_4$	73.54	49.24	28.73
$BF_{0.4}+P_5$	75.62	51.39	30.33

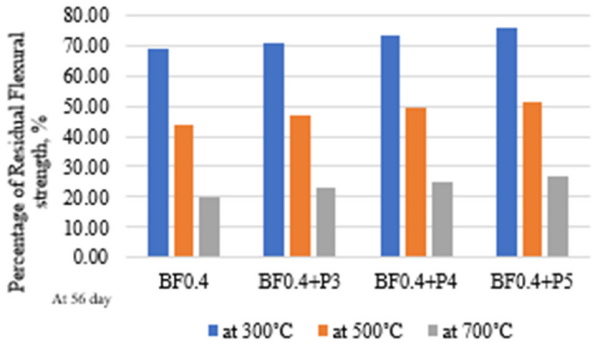

Fig. 11. Percentage of residual flexural strength after burning.

IV. CONCLUSIONS

The results showed the effect of introducing WAPB in SCC mixes, focusing on their thermal and mechanical behavior before and after exposure to high temperatures.

- The thermal conductivity coefficient value of concrete significantly increased when WAPB was added to the SCC mixes.
- The SCC samples containing WAPB that were subjected to water curing in the 28-day group exhibited a significant decrease in the compressive, splitting tensile, and flexural strength growth rates, and still, the strength values for the reference sample free of WAPB were higher.
- Incorporating BF into SCC is essential for bridging the micro-cracks and reducing the effects of volumetric alterations caused by the temperature variations while maintaining enhanced residual mechanical strength by allowing the release of capillary water vapor pressure and minimizing the explosive spalling.
- The SCC samples demonstrated a positive correlation between the increasing percentages of polymer beads and the residual compressive, splitting the tensile, and flexural strength values relative to the reference samples without polymer beads under fire flames.

REFERENCES

[1] H. K. A. Al-Obaidy, "Influence of Internal Sulfate Attack on Some Properties of Self Compacted Concrete," *Journal of Engineering*, vol. 23, no. 5, pp. 27–46, Apr. 2017, https://doi.org/10.31026/j.eng.2017.05.03.

[2] Z. K. Abbas, A. A. Abbood, and R. S. Mahmood, "Producing low-cost self-consolidation concrete using sustainable material," *Open Engineering*, vol. 12, no. 1, pp. 850–858, Jan. 2022, https://doi.org/10.1515/eng-2022-0368.

[3] N. M. Altwair, A. G. Abuzgaia, A. M. Alsharif, L. S. Sryh, S. E. A. Abdulsalam, and K. A. Swalem, "Assessing the Effects of Libyan Iron Slag on Self-Compacting Concrete Characteristics," *Engineering, Technology & Applied Science Research*, vol. 15, no. 1, pp. 19589–19595, Feb. 2025, https://doi.org/10.48084/etasr.9337.

[4] H. Awang and Z. S. Aljoumaily, "Influence of granulated blast furnace slag on mechanical properties of foam concrete," *Cogent Engineering*, vol. 4, no. 1, Jan. 2017, Art. no. 1409853, https://doi.org/10.1080/23311916.2017.1409853.

[5] B. A. Salman and M. Z. Al-Mulali, "The Effect of Nano Technology on the Properties of Sustainable Foam Concrete," *Journal of Engineering*, vol. 31, no. 6, pp. 193–203, Jun. 2025, https://doi.org/10.31026/j.eng.2025.06.10.

[6] I. F. Al-Mulla and A. S. Al-Rihimy, "The Effect of the Hydrophilic and Hydrophobic Behavior of Polymeric Fibers on Some Properties of Reactive Powder Concrete," *Engineering, Technology & Applied Science Research*, vol. 15, no. 2, pp. 21691–21694, Apr. 2025, https://doi.org/10.48084/etasr.10157.

[7] W. Z. Majeed, R. K. Aboud, N. B. Naji, and S. D. Mohammed, "Investigation of the Impact of Glass Waste in Reactive Powder Concrete on Attenuation Properties for Bremsstrahlung Ray," *East European Journal of Physics*, no. 1, pp. 102–108, Mar. 2023, https://doi.org/10.26565/2312-4334-2023-1-12.

[8] O. Benjeddou, H. Y. Katman, M. Jedidi, and N. Mashaan, "Experimental Investigation of the High Temperatures Effects on Self-Compacting Concrete Properties," *Buildings*, vol. 12, no. 6, Jun. 2022, Art. no. 729, https://doi.org/10.3390/buildings12060729.

[9] E. Gheidan, M. A. Ab. Kadir, and O. G. Aluko, "A thorough review of thermal and mechanical properties of fiber-reinforced ordinary Portland cement-SCC and pozzolanic-SCC," *Journal of Structural Fire Engineering*, vol. 16, no. 2, pp. 268–290, Feb. 2025, https://doi.org/10.1108/JSFE-08-2024-0031.

[10] A. Saand, K. A. Jamali, M. A. Keerio, T. Ali, and N. Bhatti, "Effect of Metakaolin Developed from Local Soorh on Fresh Properties and Compressive Strength of Self-Compacted Concrete," *Engineering, Technology & Applied Science Research*, vol. 9, no. 6, pp. 4901–4904, Dec. 2019, https://doi.org/10.48084/etasr.3152.

[11] Z. K. Abbas, H. A. Al-Baghdadi, and E. M. Ibrahim, "Concrete strength development by using magnetized water in normal and self-compacted concrete," *Journal of the Mechanical Behavior of Materials*, vol. 31, no. 1, pp. 564–572, Jan. 2022, https://doi.org/10.1515/jmbm-2022-0060.

[12] N. A. Memon, M. A. Memon, N. A. Lakho, F. A. Memon, M. A. Keerio, and A. N. Memon, "A Review on Self Compacting Concrete with Cementitious Materials and Fibers," *Engineering, Technology & Applied Science Research*, vol. 8, no. 3, pp. 2969–2974, Jun. 2018, https://doi.org/10.48084/etasr.2006.

[13] A. Ozodabas, "Investigation of the Effect of Basalt Fiber on Self-Compacting Concrete," *International Journal of Research - GRANTHAALAYAH*, vol. 6, no. 12, pp. 38–45, Dec. 2018, https://doi.org/10.29121/granthaalayah.v6.i12.2018.1075.

[14] S. M. Ali and H. K. Awad, "The Effect of Hybrid Fibers on Some Properties of Structural Lightweight Self-Compacting Concrete by using LECA as Partial Replacement of Coarse Aggregate," *Engineering, Technology & Applied Science Research*, vol. 14, no. 4, pp. 15002–15007, Aug. 2024, https://doi.org/10.48084/etasr.7425.

[15] Y. Gong *et al.*, "Effect of Basalt/Steel Individual and Hybrid Fiber on Mechanical Properties and Microstructure of UHPC," *Materials*, vol. 17, no. 13, Jan. 2024, Art. no. 3299, https://doi.org/10.3390/ma17133299.

[16] Z. Xue, P. Qi, Z. Yan, Q. Pei, J. Zhong, and Q. Zhan, "Mechanical Properties and Crack Resistance of Basalt Fiber Self-Compacting High Strength Concrete: An Experimental Study," *Materials*, vol. 16, no. 12, Jan. 2023, Art. no. 4374, https://doi.org/10.3390/ma16124374.

[17] J. Xu *et al.*, "Comparative study on the properties of basalt and steel fiber reinforcement waste rock concrete," *Scientific Reports*, vol. 15, no. 1, Apr. 2025, Art. no. 15103, https://doi.org/10.1038/s41598-025-99292-2.

[18] I. B. Adejuyigbe, P. C. Chiadighikaobi, and D. A. Okpara, "Sustainability Comparison for Steel and Basalt Fiber Reinforcement, Landfills, Leachate Reservoirs and Multi-Functional Structure," *Civil Engineering Journal*, vol. 5, no. 1, pp. 172–180, Jan. 2019, https://doi.org/10.28991/cej-2019-03091235.

[19] Z. Wu, X. Wang, J. Liu, and X. Chen, "13 - Mineral fibres: basalt," in *Handbook of Natural Fibres (Second Edition)*, R. M. Kozłowski and M. Mackiewicz-Talarczyk, Eds. Woodhead Publishing, 2020, pp. 433–502.

[20] M. L. Regar and A. I. Amjad, "Basalt Fibre - Ancient Mineral Fibre for Green and Sustainable Development," *EBSCO*, vol. 59, no. 4, 2016, Art. no. 321, https://doi.org/10.14502/rekstilec2016.59.321-334.

[21] V. Medina, A. Daniel, and B. Green, "Basalt and Basalt Fiber for Enhanced Control of Hazardous Materials -25679," in *ResearchGate*, Apr. 2025, [Online]. Available: https://www.researchgate.net/publication/390565143_Basalt_and_Basalt_Fiber_for_Enhanced_Control_of_Hazardous_Materials_-25679.

[22] A. Ashteyat, A. T. Obaidat, R. Qerba'a, and M. Abdel-Jaber, "Influence of Basalt Fiber on the Rheological and Mechanical Properties and Durability Behavior of Self-Compacting Concrete (SCC)," *Fibers*, vol. 12, no. 7, July 2024, Art. no. 52, https://doi.org/10.3390/fib12070052.

[23] M. Kiran Prabha, K. Vishnu Vardhan, A. S. Santhi, and G. Mohan Ganesh, "Advancements in Self-Compacting Concrete Reinforced With Basalt Fiber: A Comprehensive Review," *Engineering Reports*, vol. 7, no. 5, 2025, Art. no. e70147, https://doi.org/10.1002/eng2.70147.

[24] K. C. Onyelowe, A. M. Ebid, S. Hanandeh, V. Kamchoom, P. Awoyera, and S. Avudaiappan, "Modeling the compressive strength behavior of concrete reinforced with basalt fiber," *Scientific Reports*, vol. 15, no. 1, Apr. 2025, Art. no. 11493, https://doi.org/10.1038/s41598-025-96343-6.

[25] H. Z. Harraz, *Basalt rock fiber*. Turkey: Geology Department, Faculty of Science, Tanta University, 2019.

[26] D. Rama Seshu and A. Pratusha, "Study on compressive strength behaviour of normal concrete and self-compacting concrete subjected to elevated temperatures," *Magazine of Concrete Research*, vol. 65, no. 7, pp. 415–421, Apr. 2013, https://doi.org/10.1680/macr.12.00108.

[27] S. D. Mohammed and N. M. Fawzi, "Fire Flame Influence on the Behavior of Reinforced Concrete Beams Affected by Repeated Load,"

Journal of Engineering, vol. 22, no. 9, pp. 206–223, 2016, https://doi.org/10.31026/j.eng.2016.09.13.

[28] S. Paul, M. H. Rashid, and M. A. Rahman, "Effect of Elevated Temperature on Residual Strength of Self-Compacted Concrete," *Journal of Engineering Science*, vol. 11, no. 2, pp. 107–115, Dec. 2020, https://doi.org/10.3329/jes.v11i2.50902.

[29] M. S. Al-Lami, "Effect of elevated temperature on compressive strength of self-compacting concrete using viscocrete and silica fume," *ResearchGate*, vol. 8, no. 10, pp. 405–413, Aug. 2025.

[30] A. Alaskar, A. Albidah, A. S. Alqarni, R. Alyousef, and H. Mohammadhosseini, "RETRACTED: Performance evaluation of high-strength concrete reinforced with basalt fibers exposed to elevated temperatures," *Journal of Building Engineering*, vol. 35, Mar. 2021, Art. no. 102108, https://doi.org/10.1016/j.jobe.2020.102108.

[31] A. A. Allawi, N. K. Oukaili, and W. A. Jasim, "Strength compensation of deep beams with large web openings using carbon fiber–reinforced polymer sheets," *Advances in Structural Engineering*, vol. 24, no. 1, pp. 165–182, Jan. 2021, https://doi.org/10.1177/1369433220947195.

[32] I. F. Ahmed, "Compressive Strength of Concrete Containing Water Absorption Polymer Balls (WAPB)," *Kufa Journal of Engineering*, vol. 8, no. 2, pp. 42–52, July 2017, https://doi.org/10.30572/2018/KJE/821164.

[33] N. F. Hussen and S. D. Mohammed, "Influence of Fire-Flame Duration and Temperature on the Behavior of Reinforced Concrete Beam Containing Water Absorption Polymer Sphere; Numerical Investigation," *Journal of Engineering*, vol. 28, no. 11, pp. 67–84, Nov. 2022, https://doi.org/10.31026/j.eng.2022.11.06.

[34] N. K. Oukaili and A. A. Al-Asadi, "Analysis of Concrete Flexural Members Reinforced with Fibre Polymer," *Journal of Engineering*, vol. 16, no. 03, pp. 5569–5587, Sept. 2010, https://doi.org/10.31026/j.eng.2010.03.19.

[35] N. M. Fawzi and A. K. Weli, "Some Properties of Polymer Modified Self-Compacting Concrete Exposed to Kerosene and Gas Oil," *Journal of Engineering*, vol. 22, no. 1, pp. 31–48, Jan. 2016, https://doi.org/10.31026/j.eng.2016.01.03.

[36] A.-M. I. S. Al-Mussaue and A. H. A.-R. Al-Modhafer, "Behavior of Concrete Beams Reinforced in Shear with Carbon Fiber Reinforced Polymer," *Journal of Engineering*, vol. 17, no. 01, pp. 46–61, Jan. 2011, https://doi.org/10.31026/j.eng.2011.01.04.

[37] A. I. Said and O. M. Abbas, "Serviceability behavior of High Strength Concrete I-beams reinforced with Carbon Fiber Reinforced Polymer bars," *Journal of Engineering*, vol. 19, no. 11, pp. 1515–1530, Nov. 2013, https://doi.org/10.31026/j.eng.2013.11.10.

[38] N. M. Fawzi and A. Y. E. AL-Awadi, "Enhancing Performance of Self–Compacting Concrete with Internal Curing Using Thermostone Chips," *Journal of Engineering*, vol. 23, no. 7, pp. 1–13, June 2017, https://doi.org/10.31026/j.eng.2017.07.01.

[39] D. J. Akers *et al.*, *Guide for Structural Lightweight-Aggregate Concrete*. USA: American Concrete Institute, 1999.

[40] I. H. Jaber and W. A. Waryosh, "Effect of water-absorbent polymer balls in internal curing on punching shear behavior of bubble slabs," *Open Engineering*, vol. 14, no. 1, Jan. 2024, https://doi.org/10.1515/eng-2024-0036.

[41] J. Shi *et al.*, "The Effect of Superabsorbent Polymer on Fair-Faced Concrete Performance Based on White Cement," *Advances in Civil Engineering*, vol. 2023, no. 1, 2023, Art. no. 6615183, https://doi.org/10.1155/2023/6615183.

[42] I. F. A. Al-Mulla, A. S. Al-Rihimy, and M. F. Al-Shamaa, "Compressive Strength and Shrinkage Behavior of Concrete Produced from Portland Limestone Cement with Water Absorption Polymer Balls," *Key Engineering Materials*, vol. 857, pp. 83–88, 2020, https://doi.org/10.4028/www.scientific.net/KEM.857.83.

[43] *Iraqi Standard Specification for Portland Cement.IQS.No 5-2019*. Iraq: Iraqi Standard Specification, 2019.

[44] *Iraqi Specification for Aggregate from Natural Sources for Concrete and Building Construction, IQS.No.45.1984*. Iraq: Iraqi Standard Specification, 1984.

[45] *ASTM C1240-20 Standard Specification for Silica Fume Used in Cementitious Mixtures*. USA: ASTM International, 2020.

[46] *STM C494/C494M-17 Standard Specification for Chemical Admixtures for Concrete*. USA: ASTM International, 2017.

[47] *Iraqi Standard Materials Specification & Construction Works*. Iraq: Iraqi Standard Specification, 2004.

[48] *The European Guidelines for Self-Compacting Concrete Specification, Production and Use*. EFNARC, 2005.

[49] *BS EN 12390-3: 2019. Testing Hardened Concrete. Compressive Strength of Test Specimens*. UK: British Standards Institution, 2019.

[50] *ASTM C496 - C496M - 17 Standard Test Method For Splitting Tensile Strength of Cylindrical Concrete Specimens*. USA: ASTM International, 2018.

[51] *ASTM C293/C293M-16 (2016) Standard Test Methods for Flexural Strength of Concrete (Using Simple Beam with Center-Point Loading)*. USA: ASTM International, 2016.

[52] B. Q. Naeem and H. K. Awad, "Effect of Perlite Aggregate Replacement of Coarse Aggregate on the Behavior of SCC Exposed to Fire Flame by Using Different Cooling Methods," *Journal of Engineering*, vol. 31, no. 1, pp. 54–72, Jan. 2025, https://doi.org/10.31026/j.eng.2025.01.04.

[53] A. A. Hammadi, A. F. Izzat, and J. A. Farhan, "Effect of Fire Flame (High Temperature) on the Self Compacted Concrete (SCC) One Way Slabs," *Journal of Engineering*, vol. 18, no. 10, pp. 1083–1099, Oct. 2012, https://doi.org/10.31026/j.eng.2012.10.01.

[54] H. H. Yahy AL-Radi, S. Dejian, and H. K. Sultan, "Performance of Fiber Self-Compacting Concrete at High Temperatures," *Civil Engineering Journal*, vol. 7, no. 12, pp. 2083–2098, Dec. 2021, https://doi.org/10.28991/cej-2021-03091779.

[55] *ASTM E119-98, Standard Test Method for Fire Tests for Building Construction and Materials*. USA: ASTM International, 1987.

[56] L. Rajamony Laila, B. G. A. Gurupatham, K. Roy, and J. B. P. Lim, "Influence of super absorbent polymer on mechanical, rheological, durability, and microstructural properties of self-compacting concrete using non-biodegradable granite pulver," *Structural Concrete*, vol. 22, no. S1, pp. E1093–E1116, 2021, https://doi.org/10.1002/suco.201900470.

[57] S. Shoaib, T. El-Maaddawy, H. El-Hassan, B. El-Ariss, and M. Alsalami, "Workability and Flexural Strength of Concrete Reinforced with Basalt Macro-Fibers," in *Proceedings of International Structural Engineering and Construction*, 2022, vol. 9, no. 1, Art. no. MAT-1, https://doi.org/10.14455/ISEC.2022.9(1).MAT-32.

[58] *ASTM C1113/C1113M-09 (2013) Standard Test Method for Thermal Conductivity of Refractories by Hot Wire (Platinum Resistance Thermometer Technique)*. USA: ASTM International, 2013.

[59] Y. Wang, C. Ma, Q. Liu, Q. Zhou, and Y. Ma, "Effect of Moisture Content on Thermal Conductivity of Concretes," *China Construction Technology Group Co., Ltd*, no. 4, pp. 595–599, Sept. 2018, https://doi.org/10.3969/j.issn.1007-9629.2018.04.011.

[60] C. Chen, X. Liu, Q. Q. Zhou, and Y. L. Ma, "Effect of basalt fiber on the thermal conductivity and wear resistance of sintered WC-based diamond composites," *International Journal of Refractory Metals and Hard Materials*, vol. 105, June 2022, Art. no. 105829, https://doi.org/10.1016/j.ijrmhm.2022.105829.

[61] F. Xie, C. Zhang, D. Cai, and J. Ruan, "Comparative Study on the Mechanical Strength of SAP Internally Cured Concrete," *Frontiers in Materials*, vol. 7, Nov. 2020, https://doi.org/10.3389/fmats.2020.588130.